AIAA JOURNAL
Vol. 41, No. 10, October 2003

Gravitational Effects on Near-Field Flow Structure of Low-Density Gas Jets

Tze-Wing Yep* and Ajay K. Agrawal†
University of Oklahoma, Norman, Oklahoma 73019
and
DeVon Griffin‡
NASA John H. Glenn Research Center at Lewis Field, Cleveland, Ohio 44135

Experiments were conducted in Earth gravity and microgravity to acquire quantitative data on near-field flow structure of helium jets injected into air. Microgravity conditions were simulated in the 2.2-s drop tower at NASA John H. Glenn Research Center. The jet flow was observed by quantitative rainbow schlieren deflectometry, a nonintrusive line-of-sight measurement technique suited for the microgravity environment. The flow structure was characterized by distributions of helium mole fraction obtained from color schlieren images taken at 60 Hz. Results show that the jet in microgravity was up to 70% wider than that in Earth gravity. Experiments reveal that the global flow oscillations observed in Earth gravity are absent in microgravity. Quantitative details are provided of flow evolution as the experiment undergoes change in gravity in the drop tower.

Introduction

LOW-DENSITY jets are found in many engineering applications and natural phenomena, for example, exhaust from engines and stacks in industry, fuel leaks and accidental fires, diffusion flames, and geophysical events such as volcanic eruptions. Several recent studies[1–3] have focused on the far-field behavior of low-density jets using helium as the jet fluid. However, the near-field jet behavior has direct influence on the acoustic noise and flow development in the far field. Thus, an understanding of the flow structure in the near field of low-density gas jets is of significant fundamental importance. Subbarao and Cantwell[4] studied the near-field flow behavior of helium jets issued from a vertical tube into a coflow of air. The jets were characterized as buoyant for jet Richardson number varying between 0.5 and 6.0 in experiments [where $Ri = gd(\rho_a - \rho_j)/\rho_j U_j^2$, where g is the gravitational acceleration, d is the tube inside diameter, ρ_a and ρ_j are the freestream and jet densities, respectively, and U_j is the mass-averaged jet exit velocity]. They observed an extremely regular flowfield consisting of periodic formation and breakdown of helium-containing vortical cells. Measurements revealed large centerline velocity fluctuations and early and abrupt breakdown of the potential core. Even the large-scale structure after the breakdown repeated itself with regularity. The Strouhal number ($Sr = fd/U_j$, where f is the oscillation frequency) of the oscillating mode was independent of the Reynolds number. For $Ri > 1.0$, Sr scaled with Richardson number, indicating buoyancy-dependent instability mode. However, for $Ri < 0.5$, the Strouhal number was independent of the Richardson number. They speculated that perturbations in the airstream, for example, on the surface boundary layer outside the jet tube, were likely to dominate the flow instability and transition processes.

Pulsations in the near field of helium jets flowing into quiescent air were also observed by Hamins et al.,[5] who found that a minimum jet velocity was required to trigger the oscillations. The measured Strouhal number correlated with Froude number ($Fr = gd/U_j^2$, or inverse Richardson number), suggesting that the oscillations were buoyancy induced. They found that the Strouhal number–Froude number correlation for helium jets differed from that for flickering flames, implying differences in the buoyancy effects in nonreacting and reacting jets. Mell et al.[6] performed numerical simulations of helium jets in air and found excellent agreement between computed oscillation frequencies with those obtained experimentally by Hamins et al.[5] over a range of Froude numbers.

Experiments in naturally unstable helium jets by Cetegen and Kasper[7] extended the operating regime of Richardson numbers to those in pool fires and buoyant plumes. The oscillation frequency was represented by a correlation between Strouhal number and Richardson number for Ri varying from 1.5 to 5.0×10^4. Phase-resolved laser-Doppler velocity measurements revealed buoyant acceleration of the jet fluid accompanied with strong radial inflow of the surrounding air. A toroidal vortex ring was formed near the jet exit in the region of the highest centerline velocity. As the vortex convected downstream, it interacted with and affected the primary jet flow structure. Cetegen[8] reported similar mechanistic details of vortex formation and convection using particle image velocimetry. Flow oscillations in the near field of low-density jets have also been observed at smaller Richardson numbers (see Refs. 9–12).

Although oscillations in the near field of low-density gas jets at Richardson numbers above unity are attributed to buoyancy, no direct physical evidence has been acquired in previous experiments. Thus, the present study was conducted to investigate the effects of buoyancy on the stability and flow structure of low-density gas jets. The jet flow was quantified by helium concentration measurements obtained using the quantitative rainbow schlieren deflectometry (RSD) technique.[13] RSD is a nonintrusive optical diagnostics technique, especially suited for whole-field measurements in the microgravity environment. In the RSD technique, the optical setup is tolerant to minor mechanical vibrations or misalignments, power-consuming lasers often unsuitable for use in microgravity are not required, and seeding of the flow presenting unique challenges in microgravity is avoided. The technique has been used for measurements of concentration in helium jets[14,15] and temperature in diffusion flames in Earth gravity[16,17] and microgravity.[18] The microgravity environment was simulated in the 2.2-s drop tower facility at the NASA John H. Glenn Research Center. The experimental approach, results, and conclusions of the study are presented in the following sections.

Received 7 November 2001; revision received 18 April 2003; accepted for publication 20 May 2003.

*Graduate Research Assistant, School of Aerospace and Mechanical Engineering.
†Associate Professor, School of Aerospace and Mechanical Engineering, Room 212, 865 Asp Avenue; aagrawal@ou.edu. Member AIAA.
‡Electro-Optical Engineer, Microgravity Science Division.

Experimental Approach

The experimental setup was housed in a drop rig, 840 mm high, 960 mm long, and 400 mm wide, with a standard aluminum A frame. Al-Ammar et al.,[18] who conducted experiments with hydrogen gas jet diffusion flames in Earth gravity and microgravity, completed the initial setup. The experimental setup was modified for helium jet experiments of the present study. It consists of three major components: flow system, rainbow schlieren apparatus, and image recording system.

Figure 1 shows a schematic of the flow system. Helium gas was supplied from two 1000-cm^3 pressurized cylinders. A pressure relief valve set at 1.38 MPa (200 psig) was placed between the cylinders. The pressure regulator maintained the gas supply pressure at 690 kPa (100 psig). A calibrated mass flow meter was used to measure the helium gas flow rate. A metering valve controlled the gas flow rate. A solenoid valve was used to instantaneously activate or block the gas flow. A positioning jack was used to locate the jet tube with respect to the schlieren field of view. Jet tubes of 19.1- and 31.8-mm inside diameter were used in this study. The upstream and bend regions of the jet tube were filled with steel wool to minimize the flow nonuniformities. Steel screens were placed at the inlet and exit sections of the bend region. The straight length of the jet tube was 0.30 m because of the spatial constraints of the drop rig. Tube outside was tapered to reduce the wall thickness at the jet exit to 1.3 and 0.3 mm, for the larger and smaller diameter tubes, respectively. Unlike the studies in Refs. 6 and 7, no screen to affect flow uniformity at the jet exit was used. Thus, the present experiment represents naturally occurring conditions at the jet exit, providing true representation of such jets in practical applications.

The jet flow structure was visualized and quantified by the rainbow schlieren apparatus shown in Fig. 2. The light input to a 5-μm-wide and 3-mm-high source aperture is provided by a 150-W halogen light source connected through a 600-μm-diam fiber-optic cable. The source aperture is placed at the focal point of an 80-mm-diam, 310-mm focal length collimating lens. The collimated light rays passing through the test section are deflected by density gradients in the flowfield. The light rays are decollimated by an 80-mm-diam, 1000-mm-focal-length decollimating lens. Because of space constraints of the setup, a pair of 100-mm-diam, aluminum-coated flat surface mirrors was used to fold the rays by 180 deg. The folded light rays form the displaced image of the source aperture on a 3.5-mm-wide, computer-generated, symmetric rainbow filter, placed at the focal point of the decollimating lens. A camera lens of 75-mm focal length is used to image the test section onto the charge-coupled device (CCD) array. Schlieren images were acquired by the color camera at 60 field images per second, and digitized by a 24-bit color frame grabber installed in an onboard computer. Images were stored in tagged image file format (TIFF) at pixel resolution of 640 × 480.

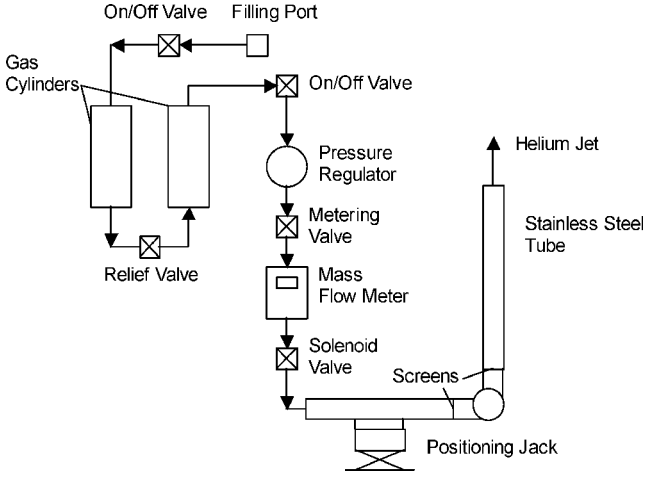

Fig. 1 Schematic diagram of the flow system.

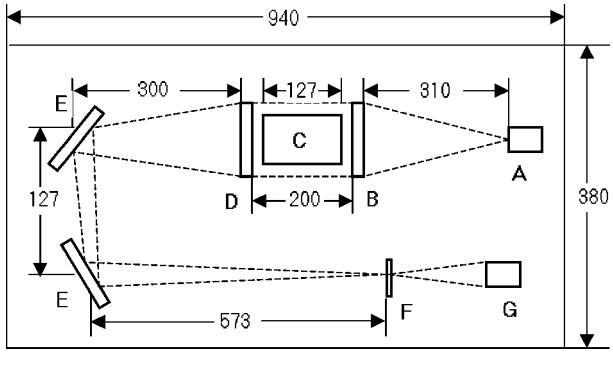

Fig. 2 Optical layout of the rainbow schlieren apparatus (all dimensions in millimeters): A, source aperture; B, collimating lens; C, test medium; D, decollimating lens; E, flat surface mirrors; F, color filter; G, and CCD array with lens.

The test sequence was automated by data acquisition and control systems resident on the computer. First, the computer fans were turned off to minimize the flow disturbances. Then, the solenoid valve was activated to turn on the jet flow. After the residual air in the jet tube was flushed out and the jet flow reached steady state, the frame grabber was activated to acquire the schlieren images. Next, the experiment was released to simulate microgravity conditions in the drop tower. After impact, the computer fans were turned on and the gas supply was turned off. After retrieving the drop rig, the image data were transferred from computer memory to an external data-storage device. For each experiment, the schlieren images were acquired for about 1.0 s in Earth gravity and 2.0 s in microgravity.

Schlieren Analysis

The angular deflection of a light ray by an axisymmetric refractive index field is given for small deflections by the following relationship:

$$\varepsilon(y) = 2y \int_y^\infty \frac{\mathrm{d}\delta}{\mathrm{d}r} \frac{\mathrm{d}r}{\sqrt{(r^2 - y^2)}} \tag{1}$$

where $\delta = (\eta - 1)$ is the refractive index difference and η is the refractive index of the test medium normalized by that of the surrounding air. In the RSD technique, the deflection angle is determined from measurements of color (or hue) in the schlieren image and the color filter calibration curve.[13,14] The refractive index difference is computed from Abel inversion of Eq. (1) expressed in discrete form as

$$\delta(r_i) = \delta(i \cdot \Delta r) = \sum_{j=i}^{NN} D_{ij} \cdot \varepsilon_j \tag{2}$$

where Δr is the sampling interval, NN is the number of intervals, and D_{ij} are geometric coefficients given in Ref. 19. In an ideal gas at constant temperature T and pressure P, the refractive index difference is

$$\delta = \frac{P}{\bar{R}T} \sum_l \kappa_l X_l M_l \tag{3}$$

where $\bar{R}$ is the universal gas constant, κ is the Dale–Gladstone constant, X is the species mole fraction, and M is the species molecular weight. The summation in Eq. (3) is taken over three species, that is, oxygen, nitrogen, and helium. Equation (3) was used to construct a table between δ and helium mole fraction, assuming nitrogen to oxygen mole ratio of 3.76 in standard air.

Measurement uncertainties arise from uncertainties in the image hue (or color) and propagate to uncertainties of angular deflection, refractive index difference, and helium mole fraction. For a given uncertainty in the image hue, the uncertainty in helium mole fraction increases exponentially toward the jet center.[14] Based on the image hue uncertainty derived from the filter calibration curve, the uncertainty of helium mole fraction is between 0.08 and 0.15 (absolute) for $r/d < 0.4$ and/or mole fractions above 0.8. Outside these

constraints, the helium mole fraction is accurate to within 8% of the measured value.

Results and Discussion

Experiments were performed to capture the flow structure in the near, mid, and far field of steady and unsteady jets in Earth gravity. Thus, at least three experiments were conducted for each test condition. In this paper, only the near-field data are presented for a steady and an unsteady jet in Earth gravity at operating conditions listed in Table 1. The jet exit Reynolds number is defined as $Re = U_j \cdot d/\nu$, where ν is the kinematic viscosity of helium.

Steady Jet (Case 1)

Figure 3 shows a sequence of contour plots of helium mole fraction during transition from Earth gravity to microgravity in the drop tower. Contour plots are shown only for one side of the jet because of the flow symmetry. Results shown are constrained to regions/values where data were considered reliable. Figure 3a shows that the jet in Earth gravity ($t = 0.0$ s) extends radially to about $r/d = 0.8$ near the tube exit. The jet width is nearly constant in the flow direction. Apparently, the radial growth of the jet shear layer between helium and air is constrained by the buoyant acceleration of the core region. Similar results were obtained by Pasumarthi,[15] who obtained detailed measurements of helium jets in Earth gravity. On entering microgravity, the jet widens at the exit where steady conditions are reached within $\frac{1}{5}$ s after the drop (Fig. 3e). The flow continues to evolve as downstream regions of the jet widen gradually. The contour plot toward the end of the drop ($t = 2.0$ s in Fig. 3f) represents steady microgravity conditions. Evidently, the jet width in microgravity is higher than that in Earth gravity by 35% at $z/d = 0.3$ and 70% at $z/d = 3.0$. In microgravity (Fig. 3f), helium mole fraction contour lines diverge away from the center, signifying a typical shear layer of a nonbuoyant jet. In contrast, the contour lines in Earth gravity (Fig. 3a) converge toward the center because of the buoyant flow acceleration. Figure 4 shows a comparison of radial profiles of helium mole fraction in Earth gravity and microgravity at $z/d = 1.5$. In microgravity, helium diffuses farther into air because of the absence of buoyancy. At this location, the jet in microgravity is about 65% wider than that in Earth gravity.

Previous studies in drop towers have raised concerns about the flow reaching steady state within the limited microgravity duration. Figure 5 shows time traces of helium mole fraction at $z/d = 1.5$ during the drop. Results show that, with the change in gravity, the jet widens initially and, thereafter, it contracts slightly before reaching steady conditions. The time delay of 0.08 s between peaks of 0.50

Table 1 Summary of test conditions

Case	d, mm	U_j, m/s	Re	Ri (in Earth gravity)	f, Hz
1	19.1	1.54	240	0.49	Nonoscillating
2	31.8	1.15	300	1.44	12.2

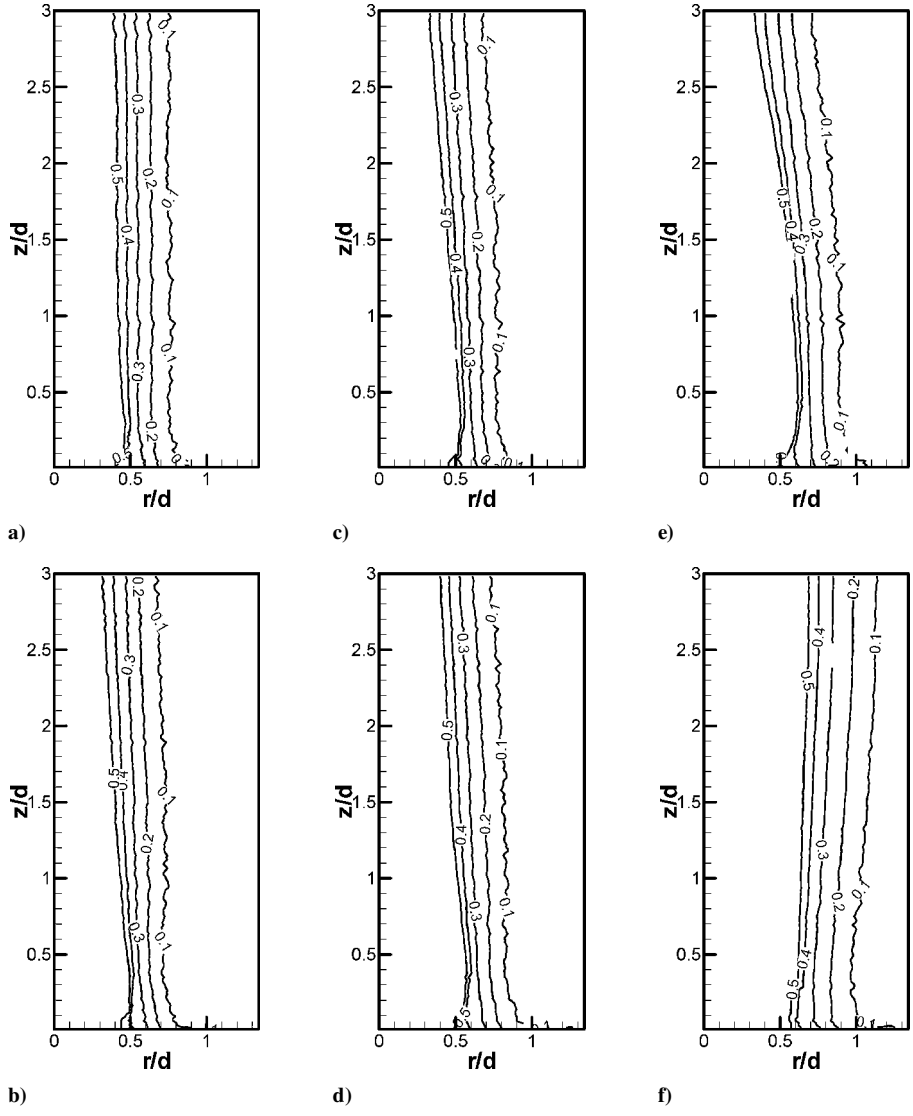

Fig. 3 Contours of helium mole fraction during transition from Earth gravity to microgravity for case 1, $d = 19.1$ mm, $Re = 240$: a) $t = 0.0$ s (denotes release of the package), b) $t = \frac{1}{30}$ s, c) $t = \frac{1}{15}$ s, d) $t = \frac{1}{10}$ s, e) $t = \frac{1}{5}$ s, and f) $t = 2.0$ s.

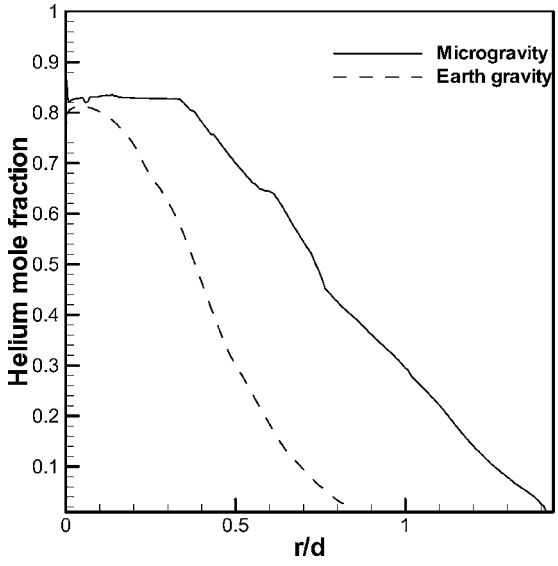

Fig. 4 Helium mole fraction in Earth gravity and microgravity for case 1, $d = 19.1$ mm, $Re = 240$, at $z/d = 1.5$.

and 0.10 helium mole fraction profiles indicates that the interior flow of the jet responds more quickly to the change in gravity. The jet expands until about $t = 0.65$ s, and steady conditions are reached throughout the jet flow after about $t = 1.0$ s. These results show that the 2.2-s duration of the drop was adequate for the experiment.

Oscillating Jet (Case 2)

For test conditions of case 2, the flow exhibited self-excited periodic oscillations in Earth gravity. Figure 6 shows a sequence of contour plots ($\frac{1}{60}$ s apart) of helium mole fraction to depict an oscillation cycle in Earth gravity. Results show that the helium mole fraction varied throughout the flowfield during the oscillation cycle. In Fig. 6a, the buoyancy-induced acceleration of light jet fluid in heavier surroundings results in contraction of the jet boundary until about $z/d = 0.35$. This process continues in the next plot (Fig. 6b), where the jet compression is observed until about $z/d = 0.75$. In the next plot (Fig. 6c), a vortex is present near $z/d = 1.4$ in between the two radial locations of the 0.50 mole fraction contour. Subsequently, the jet expands near the exit as the vortex moves downstream of the field of view. The cycle repeats itself with radial inflow of air compressing the jet core region as shown in Fig. 6f. The contour plot in Fig. 6f is similar, though not identical, to that in Fig. 6a, suggesting that the oscillation frequency is approximately 12 Hz. This

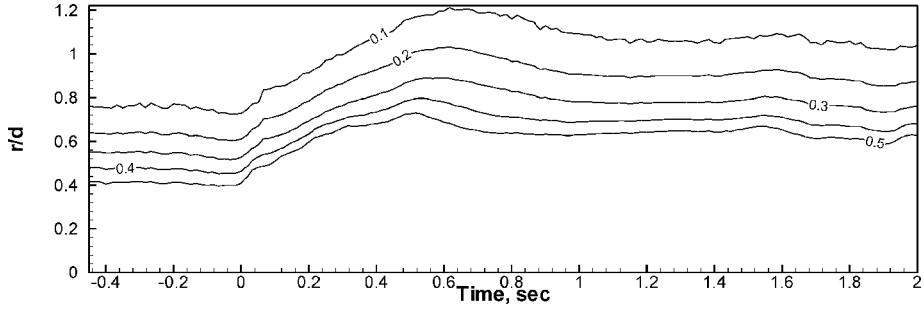

Fig. 5 Time traces of helium mole fraction during transition from Earth gravity to microgravity for case 1, $d = 19.1$ mm, $Re = 240$, at $z/d = 1.5$; time $t = 0.0$ s denotes release of the package.

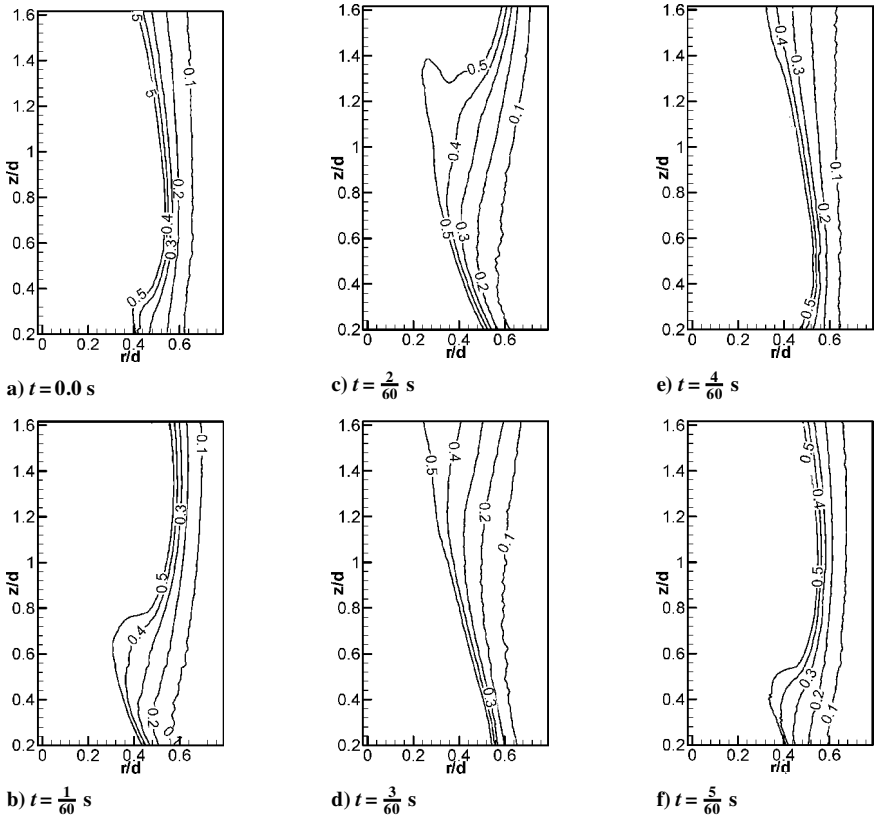

Fig. 6 Contours of helium mole fraction during a flicker cycle in Earth gravity for case 2, $d = 31.8$ mm, $Re = 300$.

is confirmed by frequency power spectra of angular deflection at several locations shown in Fig. 7. The power spectra reveal a dominant frequency of 12.2 Hz at several locations, suggesting global oscillations in the flowfield.

The evolution of the jet flow structure with change in gravity is shown in Fig. 8 by a sequence of contour plots of helium mole fraction. In Earth gravity ($t = 0.0$ s in Fig. 8a), the jet compression near the exit is accompanied with radial inflow of the surrounding air. Immediately after the drop is initiated ($t = \frac{1}{60}$ s in Fig. 8b), a vortex is observed at $z/d = 1.3$. The jet has also expanded radially near the exit region. At $t = \frac{1}{30}$ s in Fig. 8c, the vortex has moved downstream of the field of view, while the jet continues to widen near the exit region. Subsequently, the jet expands gradually in the downstream regions as steady microgravity conditions are reached. The helium mole fraction contours in microgravity are straight lines reminiscent of the nonbuoyant jet in Fig. 3f. In microgravity, the jet width exceeded the field of view of the schlieren apparatus. In the absence of a reference point in the surrounding medium (air), systematic errors were introduced during Abel inversion process in the downstream region. Thus, the contours lines in Fig. 8f did not

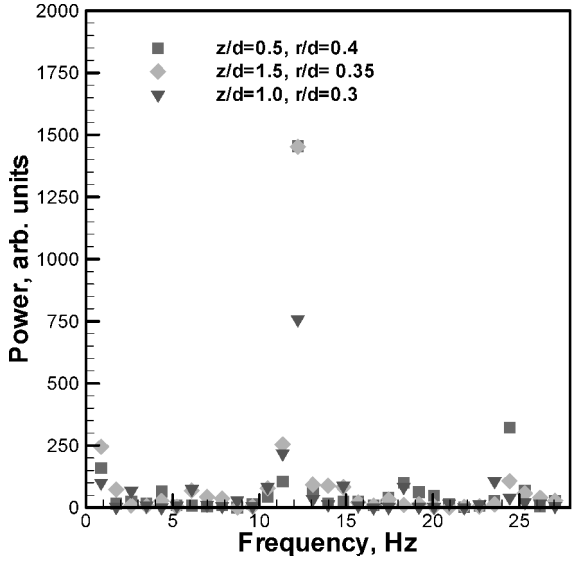

Fig. 7 Frequency power spectra in Earth gravity for various locations for case 2, $d = 31.8$ mm, $Re = 300$.

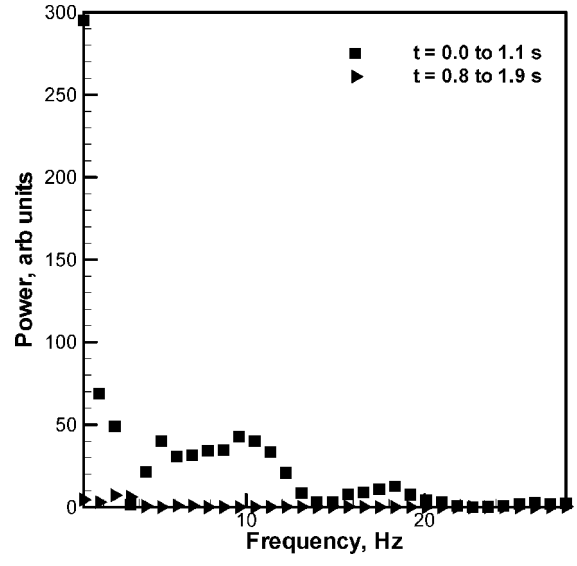

Fig. 9 Frequency power spectra for different microgravity periods for case 2, $d = 31.8$ mm, $Re = 300$, $z/d = 1.0$, and $r/d = 0.6$.

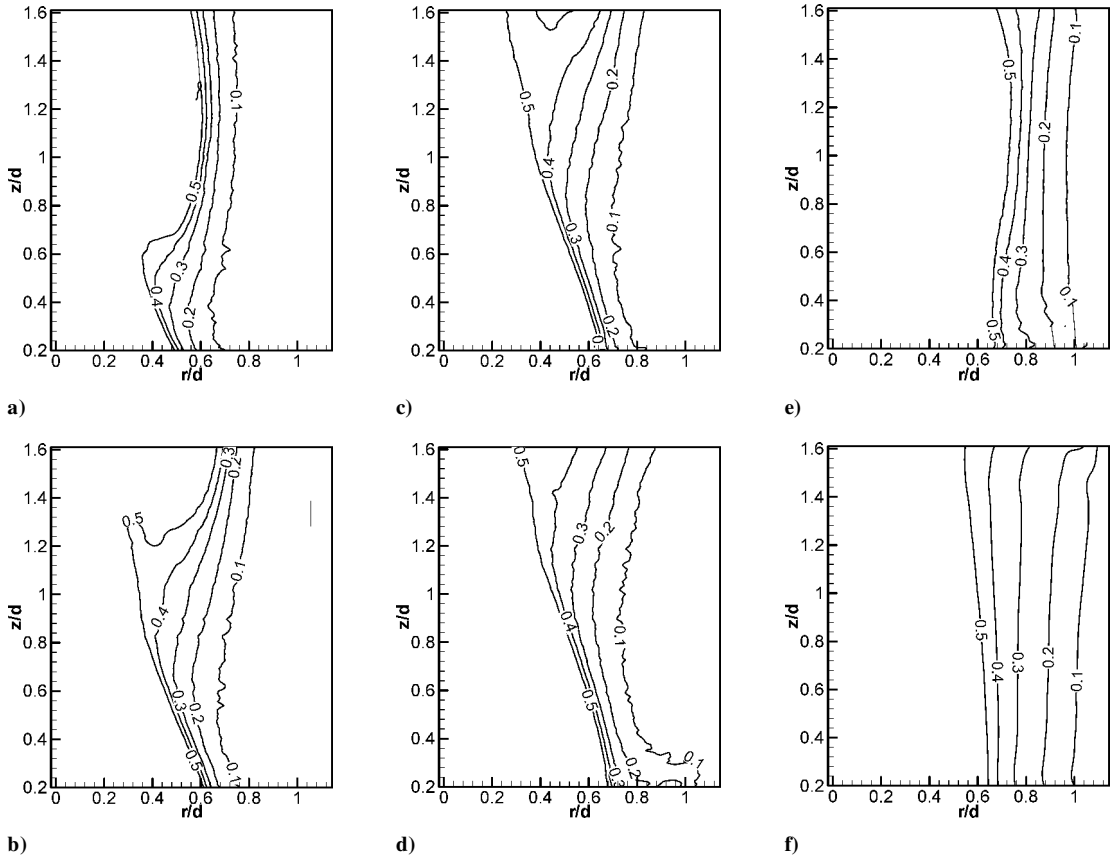

Fig. 8 Contours of helium mole fraction during transition from Earth gravity to microgravity for case 2, $d = 31.8$ mm, $Re = 300$: a) $t = 0.0$ s (denotes release of the package), b) $t = \frac{1}{60}$ s, c) $t = \frac{2}{60}$ s, d) $t = \frac{3}{60}$ s, e) $t = \frac{13}{60}$ s, and f) $t = 2.0$ s.

diverge fully as expected in nonbuoyant jets. Smaller tubes were considered to avoid this problem. However, the resulting oscillation frequency exceeded the temporal resolution of the imaging system used in this study.

Power spectra of angular deflection were obtained to assess characteristics of jet oscillations in microgravity. The analysis was performed using 1.1 s of data taken at the beginning and toward the end of the drop to distinguish initial transients from steady microgravity conditions. The power spectra in Fig. 9 show oscillations without a distinct frequency, when data at the beginning of the drop are used. Data taken at the end of the drop, however, did not produce any detectable oscillation frequency. These results provide direct physical evidence that flow oscillations in low-density jets are buoyancy induced.

The change in the jet flow during transition from Earth gravity to microgravity is shown in Fig. 10 by time traces of helium mole fraction at $z/d = 1.0$. The oscillating jet flow expands radially as it responds to the change in gravity. Figure 10 shows that the inner region of the jet expands before the outer region. Oscillations sustain during a brief initial period of microgravity, with steady conditions reached within $t = 1.0$ s. Further understanding of the jet flow during transition from Earth gravity to microgravity is obtained from Fig. 11, showing helium mole fraction profiles at different axial locations for $r/d = 0.6$. Near the jet exit at $z/d = 0.5$

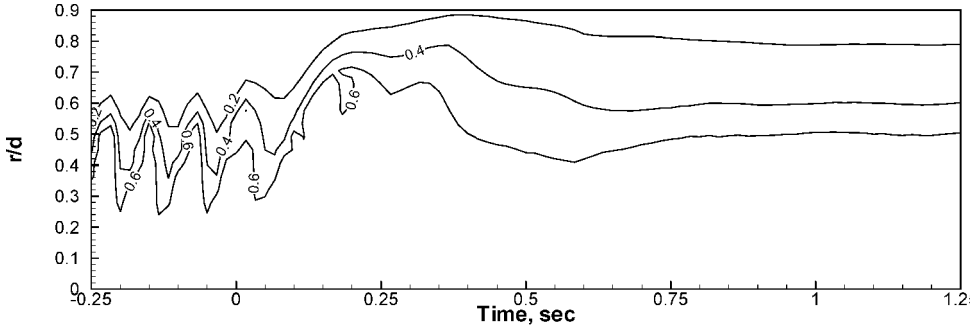

Fig. 10 Time traces of helium mole fraction during transition from Earth gravity to microgravity for case 2, $d = 31.8$ mm, $Re = 300$, and $z/d = 1.0$; time $t = 0.0$ s denotes release of the package.

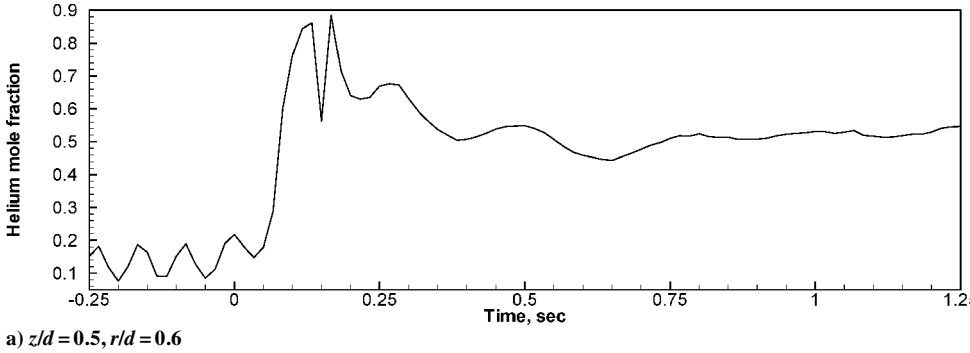

a) $z/d = 0.5$, $r/d = 0.6$

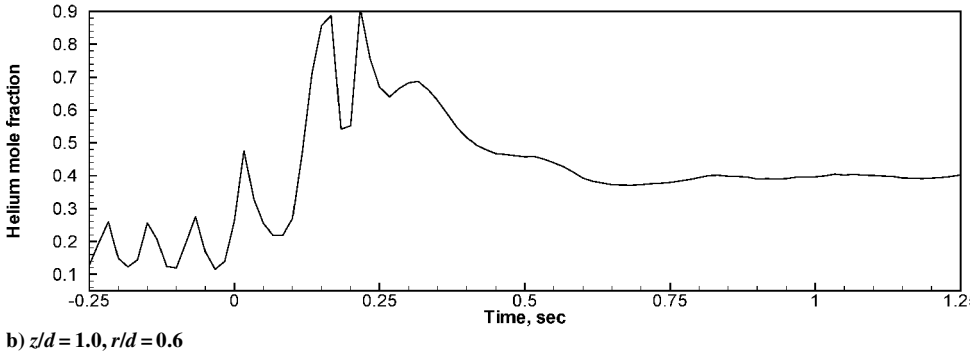

b) $z/d = 1.0$, $r/d = 0.6$

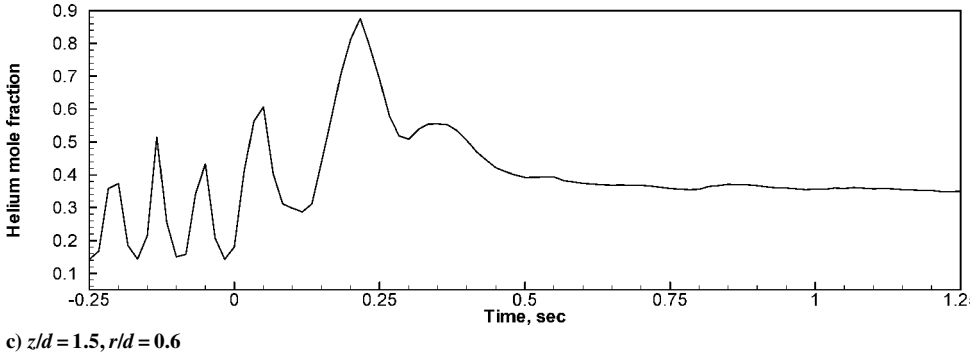

c) $z/d = 1.5$, $r/d = 0.6$

Fig. 11 Helium mole fraction during transition from Earth gravity to microgravity, time $t = 0.0$ s denotes release of the package.

(Fig. 11a), the helium mole fraction in Earth gravity varied between 0.10 and 0.20. As the jet expanded in microgravity, the helium fraction increased to about 0.90 within $t = 0.12$ s. Thereafter, the flow oscillations continued, although mean and amplitude of helium concentration decreased with time. Steady conditions corresponding to helium mole fraction of 0.55 were reached within $t = 1.0$ s. At $z/d = 1.0$ (Fig. 11b), the helium concentration peaked at $t = 0.17$ s. Subsequently, the jet oscillated briefly before reaching steady helium mole fraction of 0.40 within $t = 1.0$ s. Farther downstream at $z/d = 1.5$ (Fig. 11c), the helium concentration in Earth gravity varied between 15 and 40%. In this case, the peak helium concentration was reached at $t = 0.22$ s. The jet did not oscillate after about 0.40 s, and a steady helium mole fraction of 0.35 was reached within $t = 0.75$ s.

Conclusions

The nonintrusive, line-of-sight, RSD technique was utilized for quantitative flow measurements in the near field of buoyant and nonbuoyant helium gas jets. Results show that the radial growth of the steady jet shear layer in Earth gravity was constrained by buoyant flow acceleration of the primary jet. The jet in microgravity was 30–70% wider than that in Earth gravity. In case of a self-excited jet in Earth gravity, the flow oscillations occurred during a brief initial period as the jet flow adjusted to microgravity conditions in the drop tower. The flow oscillations were absent after steady microgravity conditions were reached in about 1.0 s. Results provide direct physical evidence, for the first time, that the flow oscillations in low-density jets in Earth gravity are buoyancy induced. Finally, the rainbow schlieren apparatus was shown to provide quantitative scalar measurements across the whole field in the microgravity environment.

Acknowledgment

This work was supported by the Physical Sciences Division of the NASA Office of Biological and Physical Research under Grant NAG 3-2388.

References

[1]So, R. M. C., Zhu, J. Y., Otugen, M. V., and Hwang, B. C., "Some Measurements in a Binary Gas Jet," *Experiments in Fluids*, Vol. 9, 1990, pp. 273–284.

[2]Richards, C. D., and Pitts, W. M., "Global Density Effects on the Self Preservation Behaviour of Turbulent Free Jets," *Journal of Fluid Mechanics*, Vol. 254, 1993, pp. 417–435.

[3]Panchapakesan, N. R., and Lumley, J. L., "Turbulence Measurements in Axisymmetric Jets of Air and Helium. Part 2. Helium Jet," *Journal of Fluid Mechanics*, Vol. 246, 1993, pp. 225–248.

[4]Subbarao, E. R., and Cantwell, B. J., "Investigation of a Co-Flowing Buoyant Jet: Experiments on the Effect of Reynolds Number and Richardson Number," *Journal of Fluid Mechanics*, Vol. 245, 1992, pp. 69–90.

[5]Hamins, A., Yang, J. C., and Kashiwagi, T., "An Experimental Investigation of the Pulsating Frequency of Flames," *Proceedings of the Combustion Institute*, Vol. 24, 1992, pp. 1695–1705.

[6]Mell, W. E., McGrattan, K. B., and Baum, H. R., "Numerical Simulation of Combustion in Fire Flumes," *Proceedings of the Combustion Institute*, Vol. 26, 1996, pp. 1523–1530.

[7]Cetegen, B. M., and Kasper, K. D., "Experiments on the Oscillatory Behavior of Buoyant Plumes of Helium and Helium–Air Mixtures," *Physics of Fluids*, Vol. 8, 1996, pp. 2974–2984.

[8]Cetegen, B. M., "Measurements of Instantaneous Velocity Field of a Non-Reacting Pulsating Buoyant Plume by Particle Image Velocimetry," *Combustion Science and Technology*, Vol. 123, 1997, pp. 377–387.

[9]Monkewitz, P. A., Bechert, D. W., Barsikow, B., and Lehmann, B., "Self-Excited Oscillations and Mixing in a Heated Round Jet," *Journal of Fluid Mechanics*, Vol. 213, 1990, pp. 611–639.

[10]Sreenivasan, K. R., Raghu, S., and Kyle, D., "Absolute Instability in Variable Density Round Jets," *Experiments in Fluids*, Vol. 7, 1989, pp. 309–317.

[11]Kyle, D. M., and Sreenivasan, K. R., "The Instability and Breakdown of a Round Variable-Density Jet," *Journal of Fluid Mechanics*, Vol. 249, 1993, pp. 619–664.

[12]Richards, C. D., Breuel, B. D., Clark, R. P., and Troutt, T. R., "Concentration Measurements in a Self-Excited Jet," *Experiments in Fluids*, Vol. 21, 1995, pp. 103–109.

[13]Greenberg, P. S., Klimek, R. B., and Buchele, D. R., "Quantitative Rainbow Schlieren Deflectometry," *Applied Optics*, Vol. 34, 1995, pp. 3819–3822.

[14]Al-Ammar, K., Agrawal, A. K., Gollahalli, S. R., and Griffin, D. W., "Application of Rainbow Schlieren Deflectometry for Concentration Measurements in an Axisymmetric Helium Jet," *Experiments in Fluids*, Vol. 25, 1998, pp. 89–95.

[15]Pasumarthi, K. S., "Full Field Scalar Measurements in a Pulsating Helium Jet Using Rainbow Schlieren Deflectometry," M.S. Thesis, School of Aerospace and Mechanical Engineering, Univ. of Oklahoma, Norman, OK, July 2000.

[16]Albers, B. W., and Agrawal, A. K., "Schlieren Analysis of an Oscillating Gas-Jet Diffusion Flame," *Combustion and Flame*, Vol. 119, 1999, pp. 89–94.

[17]Shenoy, A. K., Agrawal, A. K., and Gollahalli, S. R., "Quantitative Evaluation of Flow Computations by Rainbow Schlieren Deflectometry," *AIAA Journal*, Vol. 36, 1998, pp. 1953–1960.

[18]Al-Ammar, K., Agrawal, A. K., and Gollahalli, S. R., "Quantitative Measurements of Laminar Hydrogen Gas-Jet Diffusion Flames in a 2.2 s Drop Tower," *Proceedings of the Combustion Institute*, Vol. 28, 2000, pp. 1997–2004.

[19]Agrawal, A. K., and Albers, A. K., "Abel Inversion of Deflectometric Measurements in Dynamic Flows," *Applied Optics*, Vol. 38, 1999, pp. 3394–3398.

S. K. Aggarwal
Associate Editor